Molecular Cancer Therapeutics

Preclinical Pharmacological Evaluation of Letrozole as a Novel Treatment for Gliomas

Nimita Dave[1], Lionel M.L. Chow[2], Gary A. Gudelsky[1], Kathleen LaSance[3], Xiaoyang Qi[4], and Pankaj B. Desai[1]

Abstract

We present data that letrozole, an extensively used aromatase inhibitor in the treatment of estrogen receptor–positive breast tumors in postmenopausal women, may be potentially used in the treatment of glioblastomas. First, we measured the *in vitro* cytotoxicity of letrozole and aromatase (CYP19A1) expression and activity in human LN229, T98G, U373MG, U251MG, and U87MG, and rat C6 glioma cell lines. Estrogen receptor (ER)-positive MCF-7 and ER-negative MDA-MB-231 cells served as controls. Cytotoxicity was determined employing the MTT assay, and aromatase activity using an immunoassay that measures the conversion of testosterone to estrogen. Second, *in vivo* activity of letrozole was assessed in Sprague–Dawley rats orthotopically implanted with C6 gliomas. The changes in tumor volume with letrozole treatment (4 mg/kg/day) were assessed employing μPET/CT imaging, employing [^{18}F]-fluorodeoxyglucose (F18-FDG) as the radiotracer. Brain tissues were collected for histologic evaluations. All glioma cell lines included here expressed CYP19A1 and letrozole exerted considerable cytotoxicity and decrease in aromatase activity against these cells (IC_{50}, 0.1–3.5 μmol/L). Imaging analysis employing F18-FDG μPET/CT demonstrated a marked reduction of active tumor volume (>75%) after 8 days of letrozole treatment. Immunohistochemical analysis revealed marked reduction in aromatase expression in tumoral regions of the brain after letrozole treatment. Thus, employing multifaceted tools, we demonstrate that aromatase may be a novel target for the treatment of gliomas and that letrozole, an FDA-approved drug with an outstanding record of safety may be repurposed for the treatment of such primary brain tumors, which currently have few therapeutic options. *Mol Cancer Ther; 14(4); 857–64. ©2015 AACR.*

Introduction

Treatment of primary brain tumors remains one of the most formidable challenges in oncology. Among the various types of gliomas, grade IV astrocytoma, more commonly known as glioblastoma multiforme (GBM), is the most aggressive and fatal. Approximately, 17,000 individuals in the United States are diagnosed with GBM each year, with overall median survival of less than 2 years (1). Treatment options for GBM include surgery, radiotherapy, and chemotherapy. In general, at the time of diagnosis, most patients will undergo a maximal safe resection. Standard of care following confirmation of the pathology is radiotherapy with concurrent temozolomide, followed by temozolomide therapy for 6 months (2). Major limitations of chemotherapy for GBM include: (i) inability of many drug molecules to cross the blood–brain and blood–tumor barriers, and (ii) lack of validated new targets that may facilitate novel mechanisms for tumor treatment.

Many epidemiology studies indicate that endogenous steroid hormones including estrogens may play a role in the development of primary and metastatic brain tumors (3–5). Some of the hormonal agonists and antagonists have been investigated for the treatment of gliomas. Aromatase is a cytochrome P450 (CYP) enzyme, expressed in various tissues such as gonads, breast, and brain. Also known as estrogen synthase, aromatase is a 58-kDa protein encoded by the *CYP19A1* gene, which catalyzes the last step of biosynthesis of estrogens from androgens. In postmenopausal women, this bioconversion represents the primary source for estrogen production in peripheral tissues. As such, the use of aromatase inhibitors exemestane, anastrazole, and letrozole, that inhibit *in situ* estrogen production, has become the mainstay for the treatment of hormone-sensitive postmenopausal breast cancer patients (6). With regard to its expression in the brain, aromatase purportedly contributes to cellular proliferation, cognition, and neuroprotection (7). Estrogens synthesized locally by aromatase may influence cell survival and growth of gliomas by various estrogen-regulated mechanisms. However, clinical significance of aromatase expression for the survival and growth of brain tumors is not known. The current study represents the first attempt to delineate the role of aromatase in gliomas and its potential utility as a therapeutic target. In a previous study, we showed that the third-generation aromatase inhibitor, letrozole, easily penetrates the blood–brain and blood–tumor barriers in rats bearing C6 glioma (8). Here, we assessed *in vitro* and *in vivo* activity of letrozole against gliomas.

[1]The James L. Winkle College of Pharmacy, University of Cincinnati, Cincinnati, Ohio. [2]Cancer and Blood Disease Institute, Cincinnati Children's Hospital Medical Center, Cincinnati, Ohio. [3]Vontz Core Imaging Lab, University of Cincinnati, Cincinnati, Ohio. [4]Internal Medicine, Department of Hematology/Oncology, University of Cincinnati, Cincinnati, Ohio.

Note: Supplementary data for this article are available at Molecular Cancer Therapeutics Online (http://mct.aacrjournals.org/).

Current affiliation for N. Dave: T32 Fellow, Division of Clinical Pharmacology, Indiana University School of Medicine, Indianapolis, IN.

Corresponding Author: Pankaj B. Desai, The James L. Winkle College of Pharmacy, University of Cincinnati, 3225 Eden Avenue, Cincinnati, OH 45267-0004. Phone: 513-558-3870; Fax: 513-558-4372; E-mail: desaipb@ucmail.uc.edu

doi: 10.1158/1535-7163.MCT-14-0743

Materials and Methods

Materials

Human glioma cell lines U373MG, T98G, U251MG, LN229, U87MG, and rat glioma cell line C6 were purchased from ATCC during 2007–2010. Dulbecco modified eagle medium (Hyclone DMEM), penicillin (50 U/mL), and streptomycin (50 mg/mL) were purchased from Fisher Scientific. Normal FBS and charcoal-stripped FBS were purchased from Gemini Bio-products. Heparin sodium and MTT were purchased from Sigma Chemical Co.. Letrozole was purchased from Toronto Research Chemicals Inc. High-performance liquid chromatography (HPLC) grade solvents were obtained from Fisher Scientific. Estradiol enzyme immunoassay (EIA) kit (Catalog No. 582251) was obtained from Cayman Chemical Company. The positron emission tomography (PET) imaging agent, F18-FDG was freshly prepared and delivered on the day of the imaging by PETNET Solutions Inc.

In vitro experiments

Maintenance of tumor cell line. The human glioma cell lines U373MG, T98G, U251, LN229, U87MG, and rat glioma cell line C6 were routinely tested for mycoplasma contamination. No authentication of the cell lines was done by the authors. These cells were grown in Hyclone DMEM with 10% FBS, penicillin (50 U/mL), and streptomycin (50 mg/mL) and grown in a humidified atmosphere of 5% CO_2 at 37°C.

Real-time RT-PCR. The expression of aromatase in the cell lines was determined employing quantitative real-time reverse-transcription (RT)-PCR. As previous publications suggested we employed MCF7, ER–positive breast cancer cell line as a positive control (9), whereas the triple-negative breast cancer cell line, MDA-MB-231 served as a negative control. Total cellular RNA was isolated from lysed cells using the TRIzol reagent (Life Technologies). The concentration of purified RNA was determined by a spectrophotometer using the absorbance at 260 nm. Of the total RNA extracted, 2 μg was reverse-transcribed into cDNA using AMV-Reverse Transcriptase (Fisher Scientific). The resulting cDNA was used for real-time quantitative PCR (qPCR) analysis. qPCR assays were carried out using aromatase-specific primers. GAPDH was used as the endogenous control. The PCR mix consisted of SYBR Green PCR Master Mix (Applied Biosystems), 2 μL of cDNA, and each primer at 200 nmol/L per reaction. Real-time PCR was carried out employing ABI-7000 (Applied Biosystems) thermocycler with each cycle of PCR including 30 seconds of denaturation at 94°C, 1 minute of primer annealing at 55°C to 60°C and 2 minute of extension at 72°C. Each sample was analyzed in triplicates. The CYP19A1-specific mRNA levels were normalized to GAPDH.

Cytotoxicity assay. For the cytotoxicity assay, the cells were plated in a 96-multiwell plate at a density of 7,500 cells per well, in Hyclone DMEM media with 10% charcoal-stripped FBS, 20 U/mL penicillin, and 20 μg/mL streptomycin, at 37°C in a humidified atmosphere containing 5% CO_2. After 24-hour incubation, the cells were treated with letrozole at concentrations ranging from 0 to 100 μmol/L and control (DMSO) for a period of 1 to 3 days. Cell viability was measured employing the MTT method, reading absorbance at 570 nm in a microplate reader.

Enzyme immunoassay. Glioma cells were prepared for the assay as indicated above. After 24-hour incubation, the cells were treated with letrozole (0–100 μmol/L) and control (DMSO). The aromatase substrate, testosterone (0.1 μmol/L; volume, 10 μL) was also added to each well, and cells were incubated for 2 days. A 120 μL sample of the culture medium was removed from each well and transferred to a second 96-well tissue culture plate. The estradiol concentration in each of these wells was measured using an estradiol ELISA kit.

In vivo experiments

Female Sprague–Dawley rats (200–250 g) obtained from Charles River Laboratories, were housed individually in a room maintained at 22°C, 55% relative humidity with a 12/12-hour light/dark cycle. The rats were provided access to water and standard laboratory chow *ad libitum*. The experimental protocol was approved by University of Cincinnati Institutional Animal Care and Use Committee and all studies were conducted as per the highest international standards of animal welfare as described by Workman and colleagues (10).

Tumor cell implantation and drug treatment. C6 Glioma cells were harvested using a 0.05% Trypsin-EDTA solution and then suspended in fresh medium to obtain a final concentration of 5×10^6 cells/5 μL. The tumor cells (5×10^6 cells) were implanted into the striatum of the right hemisphere through the guide cannula, and the left hemisphere was left tumor-free to serve as a control. The tumors were allowed to grow for a period of 10 days before initiating letrozole treatment (day 0). Letrozole was reconstituted in bacteriostatic 0.9% sodium chloride (Abbott Laboratories) with 5% polysorbate 20 (Fisher Scientific) as a cosolvent and dosed at 4 mg/kg via tail vein injections on a daily basis. The untreated control group received drug-free vehicle (saline containing plus 5% polysorbate 20; 2 mL/kg). Rats were imaged on day 0 before beginning the treatment and then for the first study again on day 8 after treatment. In subsequent replicative study, imaging was performed on days 0, 5, and 8. On day 8, the rats were perfused with 1× PBS to exsanguinate tissues, followed by 4% paraformaldehyde (PFA) in 1× PBS to fix the tissues. Brain tissues were collected from the sacrificed animals for immunohistochemical analysis. For the group that received letrozole orally, the drug was constituted in the aforementioned vehicle (saline containing plus 5% polysorbate 20) and administered at 4 mg/kg dose (dissolved in 2 mL) via oral gavage.

Imaging analysis employing μPET/CT. The rats were kept fasting overnight (16 ± 2 hours) but with free access to water. The animals were anesthetized with ketamine/xylazine [70/6 mg/kg, intraperitoneal (i.p.)]. Blood glucose was measured using Bayer Contour Blood Glucose Monitoring System. F18-FDG (75 MBq) was administered by tail vein injection. The animals were kept warm for F18-FDG uptake for 30 minutes. Small-animal PET scan was then performed on a μPET scanner (Siemens Inveon). The rat was placed in the prone position on the imaging gantry and carefully positioned for a μPET/CT scan with continued warming for the duration of both scans. A CT scan was acquired for anatomical reference overlay with PET images and for PET attenuation correction for a four-minute acquisition with real-time reconstruction. The PET images were acquired over a 15-minute period and acquisition was 15 minutes and the spatial resolution in the entire field of view was determined by ordered subset

expectation maximization in 2 dimensions. Histogramming and reconstruction were applied using Siemens MicroQ software. Postprocessing was carried out with Inveon Research Workplace and general analysis and 3D visualization was used for contouring tumor volume of interest (VOI). These VOI values were considered active tumor volumes and used for further analyses.

Statistical analysis

The active tumor volumes in control (vehicle-treated) and letrozole-treated rats were expressed as mean ± SD. The pretreatment (day 0) and posttreatment (day 8) active tumor volumes were assessed for statistical differences employing single factor ANOVA followed by Student *t* test. A $P < 0.05$ was interpreted as the level of statistical significance. Data were analyzed using GraphPad Prism version 5.0 (GraphPad software).

Immunohistochemistry

Immunohistochemistry (IHC) protocol was performed as previously described (11). Brain tissues collected on day 8 (as described above in Tumor Implantation and Drug Treatment section) were fixed further by immersion in 4% PFA in 1× PBS at 4°C overnight. The tissues were processed, embedded in paraffin, and 5 μm sections were cut. Every tenth slide spanning the entire forebrain was stained with hematoxylin and eosin (H&E) to identify sections containing the tumor.

IHC was performed after microwave antigen retrieval in a citrate buffer, pH 6.0. The primary antibody and dilution used were as follows: anti-aromatase (1:200; Abcam Biochemicals, ab18995). Biotinylated goat anti-Mouse IgG antibody (Vector Labs) was used as the secondary antibody in conjunction with horseradish peroxidase-conjugated streptavidin (Elite ABC, Vector Labs). Aromatase expression was revealed with 3′3′-diaminobenzedine substrate (Vector Labs), counterstained with hematoxylin (Vector Labs), whereas Ki67 and activated caspase-3 were revealed with Vector VIP substrate (Vector Labs), counterstained with methyl green (Vector Labs).

Results

Expression of aromatase in glioma cell lines

First, we examined the CYP19A1 expression in patient-derived glioma cell lines U87MG, LN229, U373MG, U251MG, T98G, and rat glioma cell line C6 (Table 1) using real-time RT-PCR and GAPDH as the endogenous control. CYP19A1 expression was represented relative to that of the MCF7 cell line. As shown in Table 1, the expression of CYP19A1 in glioma cell lines, relative to MCF-7 cells, ranged from 1.19 (C6 rat glioma) to 2.57 (U87MG). It is noteworthy that all human cell lines tested here exhibited robust CYP19A1 expression, exceeding that in MCF-7 cells.

Table 1. CYP19A1-specific mRNA levels (indicated here relative to that in MCF-7 cell line), IC_{50} values for the observed cytotoxicity (MTT assay), and aromatase activity (enzyme immunoassay) in various human and rat glioma cell lines

Glioma cell line	Relative expression of CYP19A1	Letrozole, IC_{50} (μmol/L; MTT)	Letrozole IC_{50} (μmol/L; EIA)
MCF-7	1 ± 0	<0.1	<0.1
MDA-MB-231	0.37 ± 0.12	>100	>100
C6	1.19 ± 0.43	0.11	0.1
LN229	1.25 ± 0.27	0.96	1.12
T98G	1.35 ± 0.69	2.81	3.47
U373MG	1.69 ± 0.33	4.39	3.41
U251MG	2.03 ± 0.87	0.91	1.43
U87MG	2.57 ± 0.46	1.39	1.89

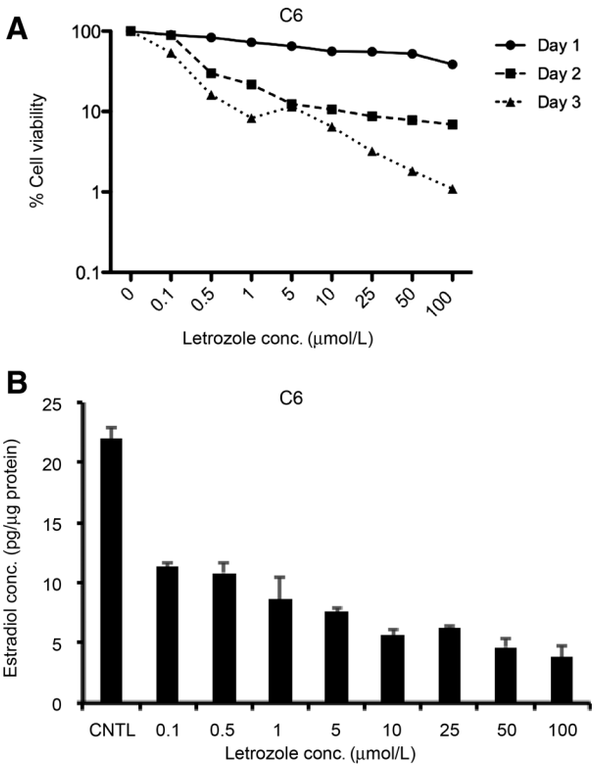

Figure 1.
A, concentration- and time-dependent cytotoxicity of letrozole in rat glioma cell line C6 in cell culture medium containing charcoal-stripped FBS.
B, concentration-dependent inhibition of aromatase activity by letrozole in rat glioma cell line C6 following treatment for 2 days in cell culture medium containing charcoal-stripped FBS.

Cytotoxicity of letrozole in glioma cell lines expressing aromatase

Next, we determined the cytotoxicity of letrozole in these cell lines as a function of time and extracellular letrozole concentrations employing the MTT assay. Letrozole concentration ranged from 0 to 100 μmol/L, and the drug treatment period ranged from 1 to 3 days. Importantly, we noted that cytotoxicity of letrozole was much higher when cells were plated in cell culture media containing charcoal-stripped serum that lacks steroids, including estrogens. The data for C6 glioma are shown in Fig. 1A and the IC_{50} values derived from such cytotoxicity profiles for each cell line employed in the study are listed in Table 1. As indicated, letrozole IC_{50} values ranged from 0.1 μmol/L for the C6 rat glioma cell line to 4.39 μmol/L for the U373MG human glioblastoma cell line.

Inhibition of aromatase activity by letrozole

To gain mechanistic insights and explore the potential link between letrozole cytotoxicity and inhibition of aromatase activity, we determined aromatase activity in these cell lines in the presence and the absence of letrozole (0–100 μmol/L). The activity of aromatase was measured as oxidative biotransformation of testosterone to estradiol. Letrozole effectively decreased estradiol

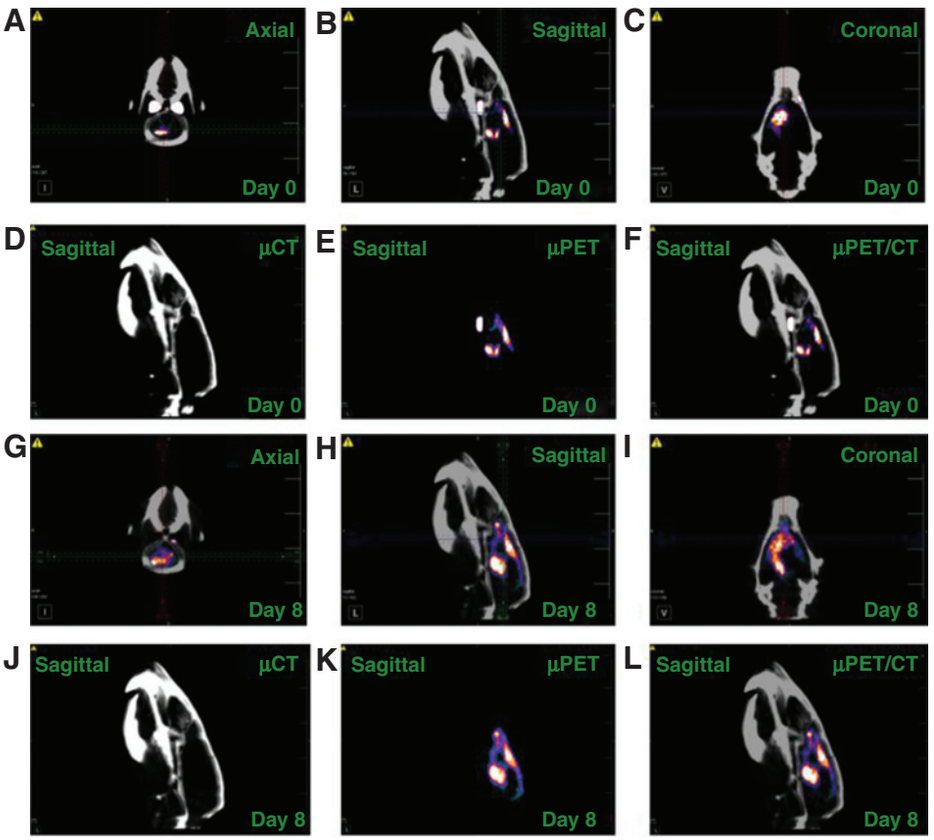

Figure 2.
μPET/CT images of a control rat with orthotopic implantation of C6 glioma. A–F, day 0 images (10 days after tumor implantation); G–L, day 8 images. A–C are axial, sagittal, and coronal views, respectively, of μPET/CT fusion images (2.1 mm thick slices). D–F are μCT, μPET, and μPET/CT fusion images of the sagittal section on day 0 of treatment. Similarly, G–I are axial, sagittal, and, coronal views, respectively, of μPET/CT fusion images (2.1 mm thick slices), whereas J–L are μCT, μPET, and μPET/CT fusion, respectively, of the sagittal sections (2.1 mm thick slices) of the same control rat on day 8 of treatment.

formation as a function of its extracellular concentration. The data for aromatase activity in C6 cells are plotted in Fig. 1B. The letrozole concentration that decreased the aromatase activity to 50% relative to control (IC_{50}) for various glioma cell lines were calculated and this data, as well as corresponding IC_{50} data from the cytotoxicity assays are included in Table 1. Overall, a good correlation ($R^2 = 0.86$) between these two parameters was observed (Supplementary Fig. S1).

In vivo efficacy of letrozole

The *in vivo* activity of letrozole was assessed using the C6 orthotopic rat glioma model. Consistent with our previous experience, the C6 tumor cells form a sizeable tumor mass in rats in 10 days (refs. 8, 12). Thus, 10 days after implantation, tumor volumes were measured in anesthetized rats employing μPET/CT (day 0 of treatment). These rats were then randomly divided into control ($n = 4$) and treatment ($n = 8$) groups. μPET/CT scans were obtained again on day 5 and/or day 8 after treatment and active tumor volumes were obtained.

Figure 2 shows μPET/CT images of a control rat with orthotopic implantation of C6 glioma on day 0 (10 days after tumor implantation) and day 8 after initiating treatment with the vehicle control. To facilitate a clear delineation of the tumor from the background we have provided the images with μPET and μCT separately and as the composite μPET/CT fusion. Furthermore, we have included the axial, sagittal, and coronal views to provide a better glimpse of the three-dimensional aspect of the tumor and the assessment of the active tumor volume. For the rat in Fig. 2, the tumor volume was 146.5 mm^3 on day 0 of treatment and increased to 192.2 mm^3 on day 8. Tumor volumes for individual rats are presented in Supplementary Table S1. Similarly, Fig. 3 shows μPET/CT images of a rat in the treatment group. For this rat, the tumor volume was 100.5 mm^3 day 0 and it decreased to 18.7 mm^3 on day 8 of letrozole treatment. This contrast between control versus treated rats was apparent consistently in each rat employed in the experiment. An increase in the tumor volume similar to that shown in Fig. 2 was apparent in all rats in the control group, with the average active tumor volume on day 0 and day 8 being 126.3 ± 13.5 mm^3 and 264.15 ± 97.2 mm^3, respectively ($n = 4$; Fig. 4A) while regression in tumor volume following letrozole treatment was observed in all the rats in the treatment group, with average active tumor volume on day 0 and day 8 being 150 ± 48.5 mm^3 and 32.75 ± 20 mm^3, respectively (Fig. 4B; Supplementary Table S1). The decrease in active tumor volume after letrozole treatment for 8 days was statistically significant ($P = 0.0001$).

F18-FDG, the PET agent used, crosses the BBB and accumulates in tissues with high turnout rate, which include tumor tissues. It is important to note that in rats, the Harderian glands, which are located in front of the brain and partly beneath the forebrain, usually show high uptake of F18-FDG (13), as observed in our μPET/CT scans (Figs. 2 and 3). However, we observed relatively lower uptake of radioactivity by the Harderian glands in the control group on day 8, potentially due to the extremely large metabolically active tumor.

As letrozole is almost completely bioavailable after oral administration and as such routinely taken orally, we also examined its activity against the C6 glioma following the oral route of

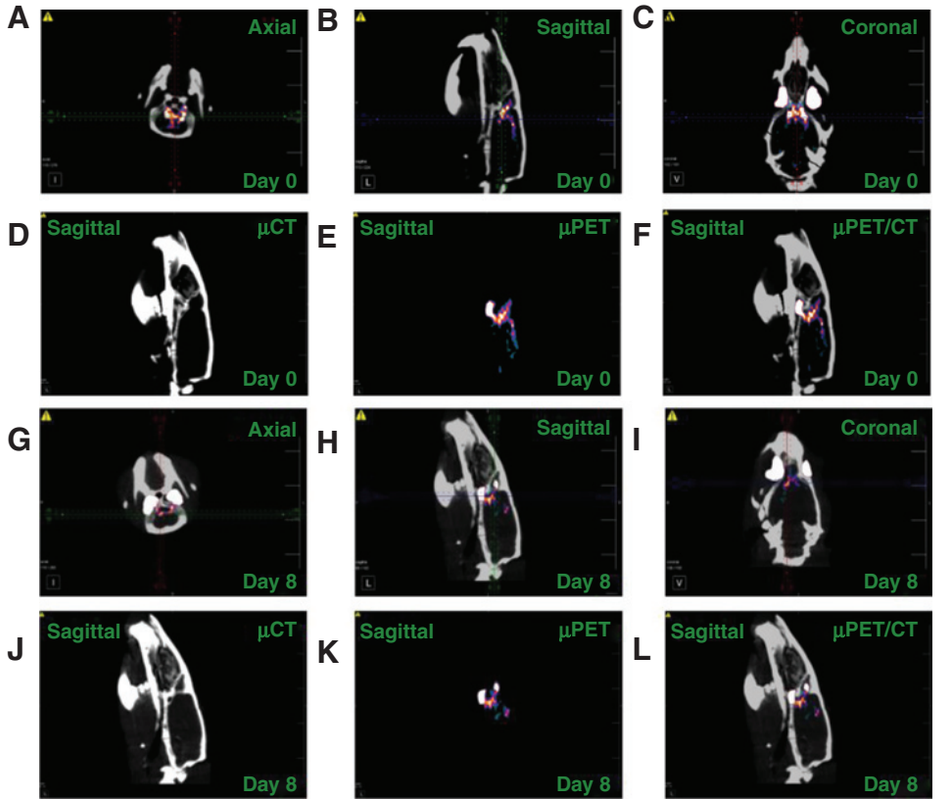

Figure 3.
μPET/CT images of a rat in the treatment group (letrozole, 4 mg/kg; tail i.v. injections) with orthotopic implantation of C6 glioma. A–F, day 0 images (10 days after tumor implantation); G–L, day 8 images. A–C are axial, sagittal, and coronal views, respectively, of μPET/CT fusion images (2.1 mm thick slices). D–F are μCT, μPET, and μPET/CT fusion images of the sagittal section on day 0 of treatment. Similarly, G–I are axial, sagittal, and, coronal views, respectively, of μPET/CT fusion images (2.1 mm thick slices) whereas J–L are μCT, μPET, and μPET/CT fusion, respectively, of the sagittal sections (2.1 mm thick slices) of the same control rat on day 8 of treatment.

administration in Sprague–Dawley rats ($N = 3$). After the initial μPET/CT scan, 10 days after the tumor implantation (day 0 of drug treatment), 4 mg/kg/d letrozole was administered daily via oral gavage. The animals were scanned again 5, 10, and 15 days after the treatment period to assess the changes in active tumor volume. The pattern of tumor regression was similar to that observed with intravenous dosing. By day 15, the tumor size shrunk by 90%. Thus, the efficacy of letrozole against C6 glioma appeared to be similar with intravenous and oral administration (data not shown here).

Overall, symptomatic differences between the control and treated groups were also quite striking and corresponded well with the differences in tumor volumes. Rats in the control group were extremely sick by day 8 and showed neurological symptoms, porphyrin staining near eyes and nose, loss of locomotor functions, and rapid weight reduction from 238.5 ± 9.7 g on day 0 to 188.3 ± 11.7 g on day 8. Unlike the rats in the control group, the rats treated with letrozole (treatment group) showed no clinical symptoms and remained healthy, with normal locomotion and normal increase in body weights throughout the treatment period of 243.8 ± 10 g on day 0 to 276.8 ± 13.2 g on day 8.

Immunohistochemistry

Expression of aromatase protein in tumors from rats of both control and treatment groups was evaluated using IHC. Rat ovary (Fig. 5A) was used as a positive control for aromatase expression (brown). Normal brain region (Fig. 5B) showed negligible aromatase expression. Brain tumor sections of rat from control group (Fig. 5C) showed high expression of aromatase, whereas tumor sections of treatment group (Fig. 5D) showed relatively very low aromatase expression.

Discussion

In recent years, the role of hormone receptors such as estrogen receptors has been evaluated for the involvement of these signaling pathways in the survival and progression of primary and metastatic tumors (3–5). The current study represents the first attempt to assess the potential role of aromatase (CYP19A1) as a novel target and letrozole, the third-generation aromatase inhibitor as an effective therapeutic agent against gliomas. The choice of this agent as the preferred aromatase inhibitor was based on outstanding record of overall safety in the clinical setting and its favorable biopharmaceutical properties such as partition coefficient (log P = 2.5), low plasma protein binding (60%), relatively quick absorption following oral administration (time to peak drug levels, 2 hours), and nearly 100% oral bioavailability (14). Furthermore, in our previous study, we noted that letrozole easily crosses the blood–brain and blood–tumor barriers in Sprague–Dawley rats implanted with C6 glioma cells. In that study, we observed that intratumoral levels of letrozole were approximately 2-fold higher than those in the normal (tumor-free) hemisphere of the rat brains (8).

All human and rat glioma cell lines tested here exhibited robust expression of CYP19A1 gene that encodes the enzyme aromatase. *In vitro* assessments suggested a good correlation between the letrozole cytotoxicity and inhibition of aromatase activity. μPET/CT imaging indicated robust reduction of tumors in female Sprague–Dawley rats. Two other lines of evidence supported the observed efficacy of letrozole. First, the tumor shrinkage in the letrozole–treated rats contrasted with the rapid tumor growth in the vehicle-treated controls and correlated well with

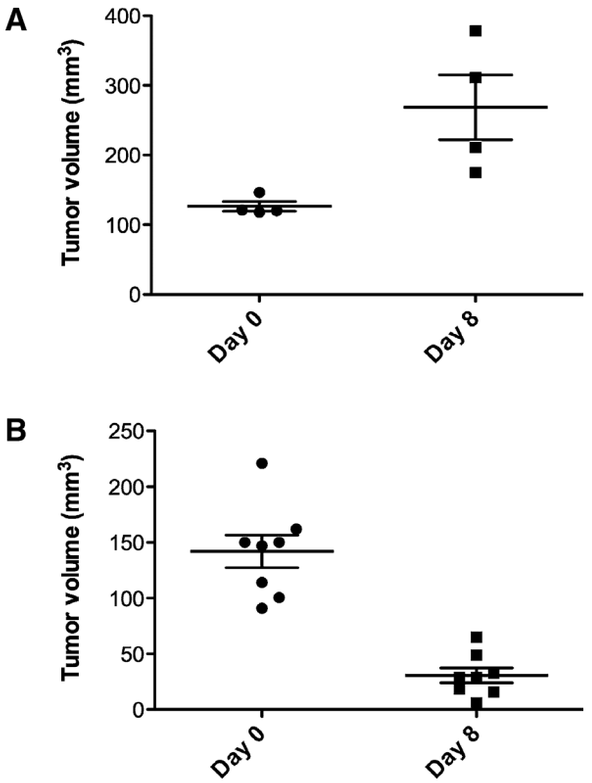

Figure 4.
Active tumor volumes (mm^3), obtained from μPET/CT scans on day 0 and day 8 for (A) control group ($n = 4$) and (B) treatment group ($n = 8$; 4 mg/kg; intravenous injection via the tail vein).

symptomatic changes. Second, immunostaining with H&E of brain sections obtained from the rats at the end of experiments helped us demarcate the tumor location. Indeed, the tumor mass was markedly reduced; in fact fairly scant to visualize, in the treated group relative to the controls.

The choice of the animal model for the *in vivo* efficacy assessment of letrozole and the letrozole dose (4 mg/kg) facilitated comparison with our previous pharmacokinetics studies where we employed microdialysis to determine the extracellular fluid (ECF) concentrations of letrozole following single dose intravenous administration (8). These *in vivo* pharmacokinetic studies showed that with the single dose of 4 mg/kg, the observed tumoral levels ranged from 0.3 to 1.25 μmol/L (peak levels), which are well above the IC_{50} of letrozole (0.1 μmol/L) observed in the *in vitro* cytotoxicity studies against the C6 glioma cells. In addition to potentially correlating this study with the previous pharmacokinetic study, we chose the experimental C6 rat model as it allows the use of an immunocompetent animal model.

A recent study underscores the emerging importance of aromatase expression in neoplastic tissues in addition to ER-positive breast carcinoma (15). This study examined CYP19A1 expression in patients with lung adenocarcinoma and suggests that aromatase expression is a prognostic factor for this disease in female subjects. In addition, in lung adenocarcinoma cell lines that had high expression of CYP19A1, exemestane, a steroidal AI, markedly reduced the survival of these cells when used in combination with erlotinib. Another study noted much higher aromatase expression in lung tumor tissue relative to those in surrounding normal tissue. These reports corroborate our findings in glioma tissues where we noted significantly higher aromatase expression in tumor region relative to the normal tissues. Furthermore, they provide additional mechanistic support for the role of aromatase inhibition in the observed activity against the glioma cells. As indicated earlier, we observed a good correlation between letrozole cytotoxicity and aromatase activity inhibition. However, it is also likely that letrozole downregulates CYP19A1 expression as immunohistochemical analyses revealed markedly lower aromatase expression in tumors from letrozole-treated animals relative to those from vehicle-treated controls. This observation has also been noted in breast carcinoma cells. Shibahara and colleagues quantified CYP19A1 mRNA levels using real-time PCR and evaluated aromatase protein levels by IHC and Western blotting in breast cancer cell lines MCF-7 and SK-BR-3 as well as clinical specimens from a neoadjuvant study before and after letrozole treatment (16). They observed a decrease in CYP19A1 mRNA levels as well as aromatase protein levels following letrozole treatment. We observe a similar pattern of decrease in aromatase protein levels in our preclinical glioma model as observed in breast cancer.

However, other mechanism(s), including those mediated by off-target effects, cannot be ruled out. The role of sex hormones such as estrogens in the etiology and progression of gliomas and the impact of estrogen depletion on gliomas is not fully delineated. For instance, while some studies suggest that estrogen has a protective role against glioma progression, other studies indicate that selective estrogen receptor modulators such as tamoxifen and 4-hydroxytamoxifen have an inhibitory effect on the growth of gliomas. Indeed, numerous experimental models of glioblastoma including those used in our study (C6, LN229, T98G, and U87MG) express estrogen receptors ERα and ERβ (5, 17, 18). In particular, it appears that ERβ signaling has tumor-suppressive activity in gliomas and ERβ agonists are currently in clinical trials for this purpose (17). The mechanism of tamoxifen cytotoxicity against gliomas is not fully elucidated, and it appears to involve inhibition of protein kinase C (19). Thus, the impact of estrogen depletion on glioma progression needs to be further clarified. Our ongoing studies are focused on seeking additional details of the mechanism(s) of cell death by letrozole. In the current study, we did not detect evidence of tumor necrosis or apoptosis (activated-caspase 3 immunoreactivity) in the remaining tumors after treatment. It is possible that at the endpoint of treatment when we removed the brain, there was no active cell death occurring in the residual tumors, or that an alternative mechanism of cell death, such as autophagy, was present. As part of our ongoing characterization of the mechanism of action of aromatase inhibition on high-grade gliomas, we will analyze tumor response at different time points after therapy and explore alternative mechanisms of cell death. These studies will enhance our understanding of mechanism(s) of resistance that may develop and of the patterns of aromatase expression and potential cross-talk with other oncogenic mutations.

The lack of mechanistic clarity notwithstanding, our results clearly demonstrate a novel approach for the treatment of aggressive gliomas with letrozole. However, we do note some of the limitation of this study. First, while we observed a marked reduction in the tumor volume in each letrozole-treated rat, there was considerable variability in the rate of tumor growth following

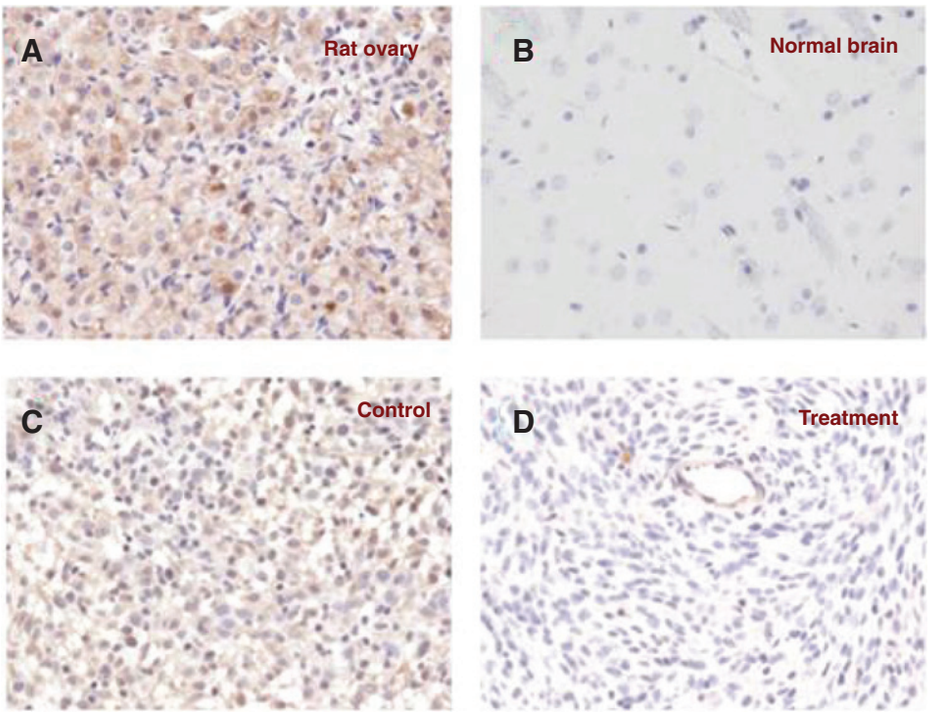

Figure 5.
Immunohistochemistry for aromatase expression in tissue sections. A, rat ovary (positive control); B, normal rat brain; C and D, tumor mass in the brains of rats implanted with C6 glioma, on day 8 (C, control group; D, treatment group).

implantation. For the control group, the mean tumor volume 10 days after implantation (on day 0) was 126.3 ± 13.5 mm^3 (range; 118–146.5 mm^3) but the rate of growth varied markedly (range; 174.9–378.4 mm^3 on day 8) with two rats exhibiting minimal growth (174.9 and 211.0 mm^3). The reasons for this variability could be that the growth of an aggressive tumor such as glioblastoma is likely to be impacted by the invasiveness of the tumor and the biologic milieu surrounding the tumor. We did observe that the tumors that were growing vertically towards the bottom of the brain were more invasive and grew to a larger extent, whereas the ones growing laterally into the olfactory bulb grew less but eventually showed severe symptoms. Second, a key consideration has to be the potential limitation of a unilateral approach of endocrine disruption by letrozole. Given the complexity of the oncogenic mutations and heterogeneity of the tumor mass, high-grade gliomas may not be sufficiently susceptible to endocrine disruption and require a combination of other drugs. Indeed studies with tamoxifen in the preclinical and clinical setting underscore the need to combine the drug with other agents, particularly temozolomide (19). Likewise, our future studies will assess the use of letrozole in combination with temozolomide and other drugs, using experimental human glioma tumor xenograft models.

In conclusion, exciting novel findings from our laboratory indicate that letrozole, an aromatase inhibitor that is widely used in the treatment of ER-positive breast tumors in postmenopausal women and has an outstanding record of safety, may also have potent efficacy in the treatment of glioma. Findings from our studies that employed multifaceted and cutting-edge tools, suggest that letrozole markedly decreased the survival of several human and rat glioma cells *in vitro*, which correlated well with the observed inhibition of aromatase enzymatic activity. Also, comprehensive pharmacodynamic studies conducted employing the state-of-the art imaging for animals (μPET/CT) showed that daily treatment with letrozole resulted in striking tumor mass reduction. Overall, our findings provide multiple lines of evidence that aromatase may be a novel target for the treatment of primary gliomas and that letrozole may be a novel therapeutic option in our arsenal to combat this dreaded disease.

Disclosure of Potential Conflicts of Interest

N. Dave and P.B. Desai have ownership interest in patents with the University of Cincinnati based on the work presented here. No potential conflicts of interest were disclosed by the other authors.

Authors' Contributions

Conception and design: N. Dave, G.A. Gudelsky, X. Qi, P.B. Desai
Development of methodology: N. Dave, L.M.L. Chow, G.A. Gudelsky, X. Qi, P.B. Desai
Acquisition of data (provided animals, acquired and managed patients, provided facilities, etc.): N. Dave, L.M.L. Chow, K. LaSance, P.B. Desai
Analysis and interpretation of data (e.g., statistical analysis, biostatistics, computational analysis): N. Dave, K. LaSance, P.B. Desai
Writing, review, and/or revision of the manuscript: N. Dave, L.M.L. Chow, G.A. Gudelsky, K. LaSance, X. Qi, P.B. Desai
Administrative, technical, or material support (i.e., reporting or organizing data, constructing databases): N. Dave, P.B. Desai
Study supervision: N. Dave, L.M.L. Chow, G.A. Gudelsky, P.B. Desai

Grant Support

This work was supported by the Molecular Therapeutics Program pilot grant from the University of Cincinnati Brain Tumor Center to the principal investigator (P.B. Desai). L.M.L. Chow is supported by a grant from the Sontag Foundation and is a St. Baldrick's Foundation Scholar.

The costs of publication of this article were defrayed in part by the payment of page charges. This article must therefore be hereby marked *advertisement* in accordance with 18 U.S.C. Section 1734 solely to indicate this fact.

Received September 4, 2014; revised January 27, 2015; accepted February 11, 2015; published OnlineFirst February 18, 2015.

References

1. Ostrom QT, Gittleman H, Farah P, Ondracek A, Chen Y, Wollinsky Y, et al. CBTRUS statistical report: primary brain and central nervous system tumors diagnosed in the United States in 2006-2010. Neuro Oncol 2013;15 Suppl 2:1–56.
2. Stupp R, Hegi ME, Mason WP, van den Bent MJ, Taphoom MJ, Janzer RC, et al., Effects of radiotherapy with concomitant and adjuvant temozolomide versus radiotherapy alone on survival in glioblastoma in a randomised phase III study: 5-year analysis of the EORTC-NCIC trial. Lancet Oncol 2009;10:459–66.
3. Silvera SA, Miler AB, Rohan TE. Hormonal and reproductive factors and risk of glioma: a prospective cohort study. Int J Cancer 2006;118:1321–4.
4. Kabat GC, Park Y, Hollenbeck AR, Schatzkin A, Rohan TE. Reproductive factors and exogenous hormone use and risk of adult glioma in women in the NIH-AARP Diet and Health Study. Int J Cancer 2011;128: 944–50.
5. Kabat GC, Etgen AM, Rohan TE. Do steroid hormones play a role in the etiology of glioma? Cancer Epidemiol Biomarkers Prev 2010;19:2421–7.
6. Connolly RM, Stearns V. Current approaches for neoadjuvant chemotherapy in breast cancer. Eur J Pharmacol 2013;717:58–66.
7. Garcia-Segura LM. Aromatase in the brain: not just for reproduction anymore. J Neuroendocrinol 2008;20:705–12.
8. Dave N, Gudelsky GA, Desai PB. The pharmacokinetics of letrozole in brain and brain tumor in rats with orthotopically implanted C6 glioma, assessed using intracerebral microdialysis. Cancer Chemother Pharmacol 2013;72: 349–57.
9. Cos S, Blask DE. Melatonin modulates aromatase activity in MCF-7 human breast cancer cells. J Pineal Res 2005;38:136–42.
10. Workman P, Balmain A, Hickman JA, McNally NJ, Rohas AM, Mitchison NA, et al. UKCCCR guidelines for the welfare of animals in experimental neoplasia. Lab Anim 1988;22:195–201.
11. Chow LM, Endersby R, Zhu X, Rankin S, Qu C, Zhang J, et al. Cooperativity within and among Pten, p53, and Rb pathways induces high-grade astrocytoma in adult brain. Cancer Cell 2011;19:305–16.
12. Apparaju SK, Gudelsky GA, Desai PB. Pharmacokinetics of gemcitabine in tumor and non-tumor extracellular fluid of brain: an *in vivo* assessment in rats employing intracerebral microdialysis. Cancer Chemother Pharmacol 2008;61:223–9.
13. Fukuyama H, Hayashi T, Katsumi Y, Tsukada H, Shibasaki H. Issues in measuring glucose metabolism of rats brain using PET: the effect of Harderian glands on the frontal love. Neurosci Lett 1998;255:99–102.
14. Lonning P, Pfister C, Martoni A, Zamagni C. Pharmacokinetics of third-generation a aromatase inhibitors. Semin Oncol 2003;30(4 Suppl 14):23–32.
15. Kohno M, Okamoto T, Suda K, Shimokawa M, Kitahara H, Shimamatsu S, et al. Prognostic and therapeutic implications of aromatase expression in lung adenocarcinomas with EGFR mutations. Clin Cancer Res 2014;20: 3613–22.
16. Shibahara Y, Miki Y, Onodera Y, Hata S, Chan MS, Yiu CC, et al. Aromatase inhibitor treatment of breast cancer cells increases the expression of let-7f, a microRNA targeting CYP19A1. J Pathol 2012;227:357–66.
17. Sareddy GR, Nair BC, Gonugunta VK, Zhang QG, Brenner A, Brann DW, et al. Therapeutic significance of estrogen receptor β agonists in gliomas. Mol Cancer Ther 2012;11:1174–82.
18. Gandhari MK, Frazier CR, Hartenstein JS, Cloix JF, Bernier M, Wainer IW. Identification and characterization of estrogen receptor- related receptor alpha and gamma in human glioma and astrocytoma cells. Mol Cell Endocrinol 2010;315:314–8.
19. Balca-Silva J, Matias D, do Carmo A, Girao H, Moura-Neto V, Sarmento-Ribeiro AB, et al. Tamoxifen in combination with temozolomide induce a synergistic inhibition of PKC-pan in GBM cell lines. Biochim Biophys Acta 2015;1850:722–32.